Research Article

The Journal of Comparative Neurology
Research in Systems Neuroscience
DOI 10.1002/cne.24055

Retinal ganglion cell topography and spatial resolving power in African megachiropterans: influence of roosting microhabitat and foraging

João Paulo Coimbra[1,2,3 *]

John D. Pettigrew[4]

Consolate Kaswera-Kyamakya[5]

Emmanuel Gilissen[5,6,7]

Shaun P. Collin[2,3]

Paul R. Manger[1]

[1] School of Anatomical Sciences, University of the Witwatersrand, 7 York Road, Parktown, 2193 Johannesburg, South Africa

[2] The Oceans Institute, The University of Western Australia, Crawley, WA 6009, Australia

[3] School of Animal Biology, The University of Western Australia, Crawley, WA 6009, Australia

[4] Queensland Brain Institute, The University of Queensland, Santa Lucia, QLD 4072, Australia

[5] Faculté des Sciences, University of Kisangani, B.P. 1232, Kisangani, Democratic Republic of the Congo

[6] Department of African Zoology, Royal Museum for Central Africa, Leuvensesteenweg 13, B-3080 Tervuren, Belgium

[7] Laboratory of Histology and Neuropathology, Université Libre de Bruxelles, B-1070 Brussels, Belgium

[8] Department of Anthropology, University of Arkansas,Fayetteville, AR 72701, USA

Running title: “Retinal topographic specializations in African megachiropterans”

Editor-in-chief: Prof. Patrick Hof

Key words: retinal topography, megachiropterans, megabats, retinal ganglion cells, stereology, spatial resolving power, visual ecology, RRID: SciRes_000114, RRID: SciRes_000116

Number of figures:7

Number of tables: 6

*CORRESPONDING AUTHOR: João Paulo Coimbra, School of Anatomical Sciences, The University of the Witwatersrand, Parktown 2193, Johannesburg, South Africa.

Email: jp.coimbra13@gmail.com

Received: Jan 30, 2016; Revised: Jun 07, 2016; Accepted: Jun 07, 2016

ABSTRACT

Megachiropteran bats (megabats) show remarkable diversity in microhabitat occupation and trophic specializations, but information on how vision relates to their behavioral ecology is scarce. Using stereology and retinal wholemounts, we measured the topographic distribution of retinal ganglion cells and determined the spatial resolution of eight African megachiropterans with distinct roosting and feeding ecologies. We found that species roosting in open microhabitats have a pronounced streak of high retinal ganglion cell density, whereas those favoring more enclosed microhabitats have a less pronounced streak (or its absence in *Hypsignathus monstrosus*). An exception is the cave-dwelling *Rousettus aegyptiacus* which has a pronounced horizontal streak that potentially correlates with its occurrence in more open environments during foraging. In all species, we found a temporal area with maximum retinal ganglion cell density (~5,000-7,000 cells/mm^2), that affords enhanced resolution in the frontal visual field. Our estimates of spatial resolution based on peak retinal ganglion cell density and eye size (~6 – 12 mm in axial length) range between ~2 and 4 cycles/degree. Species that occur in more enclosed microhabitats and feed on plant material have lower spatial resolution (~2 cycles/degree) compared to those that roost in open and semi-open areas (~3-3.8 cycles/degree). We suggest that the larger eye and concomitant higher spatial resolution (~4 cycles/degree) in *H. monstrosus* may have facilitated the carnivorous aspect of its diet. In conclusion, variations in the topographic organization and magnitude of retinal ganglion density reflect the specific ecological needs to detect food/predators and the structural complexity of the environments.

INTRODUCTION

Megachiropteran bats (megabats) represent a diverse group of nocturnal flying mammals that occupy a variety of environments ranging from open grasslands to dense tropical rainforests (Kunz and Lumsden, 2003). In bright light conditions, megachiropterans roost in a wide range of microhabitats including exposed branches in tall trees, dense foliage and caves (DeFrees and Wilson, 1988; Acharya, 1992; Langevin and Barclay, 1990; Kwiecinski and Griffths, 1999). While roosting, they appear vigilant and often open their eyes to scan for predators (Jones, 1972; DeFrees and Wilson, 1988) (Fig. 1). In dim light, megachiropterans leave their roosting sites and forage for a variety of food items including fruit, young leaves, flowers, nectar and, to a lesser extent, insects and small vertebrates (DeFrees and Wilson, 1988; Acharya, 1992; Langevin and Barclay, 1990; Kwiecinski and Griffhts, 1999). During foraging, megachiropterans display dexterity when manipulating food with their forearms and feet (Jones, 1972; DeFrees and Wilson, 1988; Kwiecinski and Griffhts, 1999), which suggests a role for vision in the guidance and control of praxic activities. Although vision plays an important role for megachiropterans, only limited information is available on their retinal topographic organization (Heffner et al., 1999; Müller et al. 2007; Heffner et al., 2008).

Vegetation structure, foraging and predator detection represent key factors that may shape the variations in the topographic distribution of retinal ganglion cells. The location and magnitude of retinal topographic specializations, formed by retinal ganglion cells, indicate how the visual field is sampled with enhanced spatial resolution (Hughes, 1977; Collin, 1999). Species that inhabit more open environments usually display more elongated patterns (streaks) of retinal ganglion cell distribution, which potentially allows for enhanced resolution across the horizon and can be particularly useful for the detection of predators (Hughes, 1977; Collin, 1999). In contrast, those species that occur in more enclosed environments generally show more concentric patterns (areas, foveas), which presumably allow for enhanced spatial resolution in a more localized region of the visual field and play a crucial role in foraging (Hughes, 1977; Collin, 1999). Among megachiropterans, previous studies have reported a combination of concentric and elongated patterns. In fruit bats

belonging to the genus *Pteropus*, variations in retinal ganglion cell density form a temporal area embedded in a weak horizontal visual streak, which potentially correlates with foraging and roosting at the top of tall trees in more open microenvironments (Beasley et al., 1985). In contrast, *Rousettus aegyptiacus* is reported to have only a temporal area with no indication of a horizontal streak, which may reflect its preference to roost in caves, whereas *Eidolon helvum* has a temporal area embedded in a weak horizontal streak potentially reflecting their occurrence in more open microhabitats (Heffner et al., 1999; 2008). Although these variations in the topographic patterns of retinal ganglion cell density appear to reflect the visual ecology of the few megachiropteran species studied to date, it is largely unknown to what extent this applies to other megachiropteran species, or whether there are shared retinal traits that may indicate a megachiropteran retinal organization blueprint.

In the present study, we examined the eyes of eight megachiropteran species with different trophic specializations and microhabitat preferences (Table 1) to investigate whether variations in the topographic distribution of retinal ganglion cells and spatial resolving power reflect ecological parameters including roosting preferences and foraging behavior. We expected that megachiropteran species that roost predominantly in open microhabitats (*E. helvum*, *E. franqueti*, *E. wahlbergi*) will have a horizontal streak, whereas those roosting in more enclosed microhabitats (*M. woermanni*, *C. argynnis*, *S. zenkeri* and *H. monstrosus*) will have a more concentric organization of ganglion cell density. Moreover, we expected that spatial resolution will reflect differential foraging needs and luminance levels across species, being higher in those species that opportunistically feed on insects and smaller vertebrates and that roost in more open microhabitats.

MATERIALS AND METHODS

Specimens

Adult specimens, comprising eight megachiropteran species, were collected in the Yoko primary rainforest, near Kisangani, Democratic Republic of Congo (*R. aegyptiacus* n = 3, *E. franqueti* n = 3, *C. argynnis* n = 3, *M. woermanni* n= 3; *H. monstrosus* n = 2, *S. zenkeri* n=1), and in coastal (*E. wahlbergii* n = 3) or inland (*E. helvum* n = 2) Kenya. Appropriate permissions to capture the animals were obtained from the University of Kisangani, DR Congo, and the Kenya National Museums, Kenya. The specimens were humanely euthanized for unrelated physiological/anatomical studies and the eyes were made available for the present investigation. The harvesting and use of these specimens was approved by the University of the Witwatersrand Animal Ethics (2008/36/1) and the University of Western Australia Ethics (RA/3/100/927) Committees.

Perfusion, tissue processing and preparation of retinal wholemounts

In the field, the specimens were intracardially perfused with 0.9% saline followed by 4% paraformaldehyde in 0.1M phosphate buffer (PB, pH=7.2-7.4). After perfusion, orientation marks were made on the dorsal aspect of the cornea using a portable cautery device before the eyes were enucleated (Coimbra et al., 2013). Extraocular tissue was carefully removed and the axial length of the excised eyes measured using a digital caliper. Whole eyes were then post-fixed in the same fixative solution for 24 h. Fixation was stopped by transferring the eyes to 0.1M PB (pH= 7.2-7.4) containing 0.1% sodium azide.

In the laboratory, retinal wholemounts were prepared and processed following standard methods (Stone, 1981; Coimbra et al., 2006). Briefly, the cornea and vitreous were removed and the retinas were dissected by making radial cuts from the periphery to the center of the eyecup. Sclera pieces were then removed and the retina was finally detached by severing the optic disc at its base using a scalpel blade. Remnants of retinal pigment epithelium

attached to the retinal wholemounts were bleached with 3% hydrogen peroxide in 0.1M PB for approximately 12 hours at room temperature (Coimbra et al., 2009).

Retinal wholemounts were mounted vitreous side up onto a gelatinized slide for staining of cells in the retinal ganglion cell layer using the Nissl method. To improve the adherence of the retinal wholemount to the slide and to augment the differentiation of ganglion cells during the staining procedure, retinal preparations were incubated in formaldehyde vapors at room temperature overnight (Stone, 1981). Retinal wholemounts were then rehydrated, stained for 5 minutes with an aqueous solution of 0.1 % of cresyl violet (Sigma), dehydrated in an ethanol series, cleared in xylene and finally mounted with Entellan New (Merck) (Coimbra et al., 2006). As the preparations were attached to the slides during all staining steps, shrinkage was considered to be negligible and confined to the borders of the *ora serrata* and the edges of radial cuts (Wässle et al., 1981; Peichl, 1992).

Stereological assessment of the total number and topographic distribution of photoreceptors and retinal ganglion cells

Using the optical fractionator method (West et al., 1991) with modifications for the use in retinal wholemounts (Coimbra et al., 2009), we estimated the total number and the topographic distribution of retinal ganglion cells in megachiropterans. Briefly, the retina was considered as one single section and therefore the section sampling fraction (ssf) was 1. As the retinal ganglion cell layer in all megachiropterans examined comprises a single layer of neurons, the optical disector height was the same as the thickness of the ganglion cell layer at all eccentricities, giving a thickness sampling factor (tsf) of 1. Therefore, only the area sampling fraction (asf), which is the ratio between the counting frame and the sampling grid, was used to estimate the total number of retinal ganglion cells according to the following algorithm:

$N_{total} = \Sigma Q \times 1/asf$,

where ΣQ is the sum of total neurons counted (West et al., 1991).

The outlines of retinal wholemounts were digitized using a 4 x/NA 0.13 objective on a microscope (Olympus BX50) equipped with a motorized stage (MAC200; Ludl Electronics Products, USA) and connected to a computer running Stereo Investigator software (http://www.mbfbioscience.com, RRID: SciRes_000114). The retinal ganglion cell layer was outlined close to the limits of the retinal borders (at the *ora serrata*) and along the radial cuts, but excluding other retinal layers that can be seen in transverse view after wholemounting. The outline of the base of the optic disc was subtracted from the total retinal wholemount area.

We used different sampling strategies to map the topographic distribution of ganglion cells in retinal wholemounts of the megachiropterans examined to account for differences in retinal area and neuronal density gradient (Table 1). Under macroscopic examination, we noticed that the retinal ganglion cell layer showed homogeneous staining indicating a shallow density gradient, so we opted to sample the entire retina with a single grid and counting frame size. Upon identification of the highest density region, we used a high frequency sampling scheme to confirm the magnitude and location of the peak density estimates. Sampling grids were placed in a random, uniform and systematic fashion covering the area of each contour. At each sampling site, only retinal ganglion cells that lay entirely within the counting frame or that intersected the acceptance lines without touching the rejection lines were counted (Gundersen, 1977). These stereological parameters were chosen on the basis of pilot experiments to achieve a Schaeffer coefficient of error (CE) < 0.1, which is deemed appropriate in the present study because variance introduced by the counting procedures contribute very little to the observed group variance (Glaser and Wilson, 1998; Slomianka and West, 2005).

To distinguish ganglion cells from amacrine and glial cells, we used well established cytological criteria proposed by Hughes (1981) and validated in a range of mammal species (Wong et al., 1986; Silveira et al. 1989a; Silveira et al., 1989b; Peichl, 1992; Mass and

Supin, 1992; Silveira et al., 1993; Mass and Supin, 2003; Hanke et al., 2009; Mass and Supin, 2010; Coimbra et al., 2013; 2015). Cell profiles showing a polygonal soma with dense accumulations of Nissl substance in the cytoplasm, an eccentric nucleus and a prominent nucleolus were classified as retinal ganglion cells (Fig. 2). Smaller, rounder and more palely stained profiles, with no evident Nissl substance in the cytoplasm were classified as amacrine cells (Fig. 2). Darkly stained profiles displaying a small, round or slightly elongated cell body were recognized as glial cells (Fig. 2). These cytological criteria were consistent at all eccentricities and were unambiguously applicable in low, moderate and high density regions of the megachiropteran retinas (Fig. 2). Because retinal ganglion cells were reliably identified at all eccentricities, we opted to exclude other cell types from the counting procedures.

To map the topographic distribution of retinal ganglion cells in the retinas of megachiropterans, cell counts at each sampling site were converted to an equivalent cell density per square millimeter. We used Arcview 3.2 software (http://www.esri.com, RRID: SciRes_000116) to construct topographic maps depicting the distribution of ganglion cells in the megachiropteran retinas using the spline interpolation method (Coimbra et al., 2006).

Photomicrographs were obtained using a digital camera (Microfire, Optronics, CA) coupled to a Stereo Investigator system. Digital photomicrographs were processed using Adobe Photoshop CS2 (San Jose, CA) for scaling and minor adjustment of the levels of brightness and contrast.

Anatomical estimation of spatial resolving power

Spatial resolving power of the eye of megachiropterans was estimated using anatomical methods. The posterior nodal distance (PND) was indirectly estimated by multiplying the axial length by 0.52 according to the ratio between PND: axial length described for nocturnal species (Pettigrew et al., 1988). All megachiropterans examined show peak activity after sunset and return to their roosting sites before sunrise (Nowak, 1994).

To estimate the retinal magnification factor (RMF), which represents the distance in retinal surface that subtends one degree, we used the equation (Pettigrew et al., 1988):

$$RMF=2\pi PND/360$$

We adopted two approaches to estimate the highest spatial frequency of the megachiropteran eye. In the first, we considered that retinal ganglion cells in the peak region are organized in an approximate square lattice and estimated the linear density (cells/mm) by calculating the square root of the peak density (cells/mm^2). According to the sampling theorem, as the sampling density is twice the threshold, we divided the linear density by 2. This value was then multiplied by RMF to obtain the highest spatial Nyquist frequency (Pettigrew et al., 1988). In the second approach, we assumed that the retinal ganglion cells in the peak region were organized in a triangular lattice (often described as a hexagonal lattice) because this arrangement allows for the minimum center-to-center spacing among cells (Williams and Coletta, 1987). We used the retinal ganglion cell peak density (D) to estimate the highest spatial frequency as determined by the Nyquist limits of spatial resolution according to the following equation (Snyder and Miller, 1977; Williams and Coletta, 1987):

$$f_N = 0.5 \times RMF \times (2D/\sqrt{3})^{1/2}$$

Anatomical estimates of spatial resolving power using the total peak density of retinal ganglion cells should be considered as upper limits of retinal resolution because it is not known whether all retinal ganglion cells in the peak region are involved in fine discrimination tasks (Wässle, 2004; Reuter and Peichl, 2008).

To relate behavioral significance to our estimates of spatial resolving power (SRP), we calculated the minimum resolvable distance that the megachiropteran species examined can spatially resolve objects (food items or predators) located at distances relevant to their ecological context. Assuming that the object sizes are about twice the threshold, we calculated the minimum separable angle (α) (Marshall, 2000):

α=1/SPR

Then, using the trigonometric relationships between the minimum separable angle (α) and a presumed distance relevant for foraging and predator detection (D), we estimated the minimum target size (MTS) that a megachiropteran can spatially detect objects following the equation below:

D= MTS/tan α

For these estimates, we assumed optimal contrast and luminance conditions.

RESULTS

The tapetum lucidum of megachiropterans

Examination of the eye fundus of all megachiropteran species examined revealed the presence of a bright yellow tapetum lucidum covering almost the whole extension of the dorsal hemisphere as shown in two representative species, *E. franqueti* and *H. monstrosus* (Fig. 3). In all species, the choroid exhibits dark pigmentation in the ventral part of the retina and the far periphery of the dorsal hemisphere (Fig. 3).

Stereological assessment of the total number and topographic distribution of retinal ganglion cells

The retinal area in the megachiropteran species studied ranges from ~40-50 mm^2 (*M. woermani* and *S. zenkeri*) to ~200 mm^2 (*H. monstrosus*). The remaining species have retinal areas ranging between ~90 and 140 mm^2 (Table 3). The estimated total number of retinal ganglion cells varied from ~90,000 (*M. woermanni* and *S. zenkeri*) to ~ 300,000 (*H. monstrosus*). The total numbers of retinal ganglion cells in *C. argynnis* (~130,000) and *R. aegyptiacus* (~160,000) fall closer to the lower estimates, whereas *E. wahlbergi* and *E. franqueti* show intermediate estimates (~200,000) within the range. Estimates of ~280,000

retinal ganglion cells in *E. helvum* fall closer to the maximum numbers estimated for *H. monstrosus* (Table 3). The mean Schaeffer CE for our estimates of total number of retinal ganglion cells is low, ranging between 0.028 and 0.036 (Table 3). The variance introduced by methodological procedures should not be higher than 50% of the observed group variance, giving a CE^2/CV^2 ratio of less than 0.5 (Slomianka and West, 2005). We estimated CE^2/CV^2 ratios below this value for *E. wahlbergi* (0.07), *M. woermani* (0.49) and *C. argynnis* (0.15) (Table 4). However, although the ratios of 1.55 for *E. franqueti* and 1.84 for *R. aegyptiacus* were greater than 0.5, they are not indicative of variability introduced by the stereological procedures (mean CE = 0.050), but instead they reflect lower interindividual variability compared to the other species (Table 3). We could not determine the CE^2/CV^2 ratio for *E. helvum* and *S. zenkeri* because our samples for these species consisted of two and one specimen respectively.

Topographic mapping of retinal ganglion cell densities revealed a combination of concentric and elongated patterns in the megachiropteran species examined (Fig. 4, 5). In all species, we found a temporal area defined by concentric isodensity lines between 3,500 and 5,500 cells/mm^2 (Fig. 4, 5). Within the limits of these isodensity lines, the maximum density of retinal ganglion cells ranges from ~5,000 in *E. franqueti* to ~7,000 cells/mm^2 in *E. helvum* (Table 3). In megachiropteran species that occur predominantly in more open microhabitats (*E. helvum*, *E. franqueti* and *E. wahlbergii*) and the cave-dwelling *R. aegyptiacus*, we found that isodensity lines between 2,000 and 2,500 cells/mm^2 taper across the retinal equator towards the nasal periphery delineating a weak horizontal streak (Fig. 4). Towards the far periphery, isodensity lines between 1,000 and 1,500 cells/mm^2 are more concentrically organized (Fig. 4).

In species that occur predominantly in more closed microhabitats (*M. woermanni*, *S. argynnis*, *S. zenkeri* and *H. monstrosus*), we found that isodensity lines surrounding the temporal area occur in the same range of 2,500 – 5,000 cells/mm^2 for species described above (Fig. 5). These species show a more symmetric and concentric topographic organization of retinal ganglion cell density (Fig. 5). In *M. woermanni*, *S. argynnis*, and *S.*

zenkeri, isodensity lines of 2,500 – 3,000 cells/mm^2 show a slight elongation towards the nasal part of the retina, indicating the presence of a loosely-organized horizontal streak (Fig. 5). In contrast, in *H. monstrosus*, the isodensity line of 2,000 cells/mm^2, which immediately surrounds the temporal area show a more vertical rather than horizontal elongation (Fig. 5). Towards the far periphery, isodensity lines (1,500 - 2,000 cells/mm^2 in *M. woermanni*, *S. argynnis*, and *S. zenkeri*; 1,000 – 1,500 cells/mm^2 in *H. monstrosus*) are more concentrically organized (fig. 5).

Anatomical spatial resolving power

We found that megachiropterans that occur predominantly in open environments (*E. helvum*, *E. franqueti*, *E. wahlbergi*) have larger eyes (~8.5-9.5 mm in axial length) compared to most species that occur predominantly in more enclosed environments (~6 mm in axial length; *M. woermanni*, *C. argynnis*, *S. zenkeri*). However, our estimates of axial length were larger for two species favouring more enclosed environments (~8 mm for *R. aegyptiacus*; ~12 mm for *H. monstrosus*) (Table 5). With this range of eye sizes, we estimated posterior nodal distances ranging between ~3 mm and 6 mm and retinal magnification factors between 0.055 and 0.107 mm/degree for *S. zenkeri* and *H. monstrosus* respectively. Using maximum retinal ganglion cell density in the temporal area, we estimated the upper limits of spatial resolving power for square and triangular lattices ranging between ~2 and ~4 cycles/degree (Table 5).

For species with the lowest (~2 cycles/degree) and highest (~4 cycles/degree) spatial resolving power we estimated a minimum separable angle between ~ 0.45° (*M. woermanni*, *S. zenkeri* and *C. argynnis*) and ~0.25° (*E. helvum* and *H. monstrosus*). For species with intermediate (~3 cycles/degree) spatial resolving power, we calculated a minimum separable angle of ~0.33° (*R. aegyptiacus*, *E. wahlbergii* and *E. franqueti*) (Table 6). At a presumed foraging distance of 1 m from the megachiropteran species, these angles translate into minimum target sizes ranging between ~8 mm (species with lowest resolution) and ~ 4 mm

(species with highest resolution). At the same distance, for species with intermediate resolution the estimated minimum target size is ~6-5 mm. At a distance presumably relevant for predator surveillance (~10 m), minimum target sizes range between ~ 4 cm (species with highest resolution) and ~8 cm (species with lowest resolution). For species with intermediate resolution the estimated minimum target size at distances of 10 m is ~6-5 cm (Table 6). These estimates indicate that, at these presumed distances, objects larger than the minimum target sizes can be spatially detected given optimal conditions of contrast and luminance.

DISCUSSION

The main results of our study show that the topographic distribution of retinal ganglion cells generally reflects variations in roosting microhabitat occupation and foraging for most African megachiropterans examined (Fig. 6). We found that species that roost in relatively open microhabitats show more elongated patterns of retinal ganglion cell distribution, whereas those species that occupy enclosed microhabitats have more concentric patterns; however, in contrast to previous reports, we found that the cave-dwelling *R. aegyptiacus* has a horizontal streak. All species studied have a temporal area of high ganglion cell density affording upper limits of spatial resolving power between ~2 and ~4 cycles/degree.

Microhabitat occupation and the topographic distribution of retinal ganglion cells in African megachiropterans

Because some megachiropteran species show preference to roost in more open, whereas others favour more enclosed microhabitats, we predicted that the topographic distribution of retinal ganglion cells would reflect these roosting preferences. In general, our findings support this prediction. In *E. helvum*, *E. franqueti* and *E. wahlbergi*, our finding of a horizontal streak of high ganglion cell density is consistent with their preferred roosting sites

in more open microhabitats. Although *E. helvum* roosts in a variety of microhabitats including lofts in caves and rocks, this species commonly aggregates in exfoliated branches of trees up to 20 m in height (Jones, 1972; DeFrees and Wilson, 1988). *E. franqueti* and *E. wahlbergi* both occur in savanna woodlands, grasslands and forest margins (Jones, 1972; Acharya, 1992; Nowak, 1994). In these microhabitats the sparse or more open vegetation structure makes these species more vulnerable to predation, hence panoramic surveillance of the horizon is useful. In fact, *E. helvum* and *E. franqueti* remain vigilant even in bright light conditions with eyes usually open and ears in constant motion (Jones, 1972; DeFrees and Wilson, 1988). Therefore, the horizontal streak of high retinal ganglion cell density in megachiropterans may afford increased resolution across the horizon, potentially assisting with predator surveillance.

Our finding of a generally concentric organization of the topographic distribution of retinal ganglion cell densities in predominantly forest-dwelling species (*M. woermanni*, *C. argynnis*, *S. zenkeri* and *H. monstrosus*) gives further support to our prediction that microhabitat occupation represents an important driving force shaping the topographic distribution of retinal ganglion cells. However, although all the forest-dwelling megachiropteran species studied here show a generally concentric organization of retinal ganglion cell densities, we found that all species — with exception of *H. monstrosus* — show an elongation across the nasotemporal equator, suggesting the presence of a weak horizontal streak. Although *M. woermanni*, *C. argynnis* and *S. zenkeri* occur in forest habitats roosting under dense foliage at different strata of the vegetation, they also may use, to some degree, more open environments while foraging (Weber et al., 2009). For example, Weber et al. (2009) have reported the obligatory nectarivorous *M. woermanni* drinking nectar from banana inflorescences outside forests. In addition, Fahr (2014) reported that although *S. zenkeri* inhabits predominantly primary forests it also occurs in more open environments such as forest fringes, forest gaps and cleared areas. Therefore, the presence of this weak horizontal streak may reflect the transitional use of more open environments by these forest-dwelling megachiropteran species.

In contrast, we found no indication of a horizontal elongation in the topographic distribution of retinal ganglion cell density in forest-dwelling *H. monstrosus*. This represents an interesting deviation from the topographic patterns we found for the other forest-dwelling species. Although, *H. monstrosus* roosts in forest environments between 20-30m above the forest floor, or in relatively more open vegetation habitats such as mangroves and palm forests (Langevin and Barclay, 1990), the more concentric topographic organization of ganglion cell densities in their retinas may reflect their roosting beneath dense foliage cover (Langevin and Barclay, 1990), which may have obviated the need for increased visual sampling across the horizon.

Many species of megachiropterans exhibit sophisticated levels of dexterity in manipulating food items with their thumbs and feet (Jones, 1972; DeFrees and Wilson, 1988). Our finding that all species of megachiropterans examined in the present study have a concentric increase of density of retinal ganglion cells in the temporal part of the retina corroborates our prediction that they would have a temporal area. The use of thumbs and feet to assist with manipulation of food has been reported for *E. helvum*, which occasionally hang by their thumbs and manipulate food with their feet and mouth (Jones, 1972; DeFrees and Wilson, 1988). In addition, Jones (1972) reported that *E. franqueti* can manipulate food items using one foot, mouth and wrists, for which the presence of a temporal area would facilitate visual sampling with increased resolution in the frontal visual field. Moreover, *E. franqueti* also uses thumbs and feet during non-flight locomotion for short distances between branches and leaves (Jones, 1972). In this case, a temporal area would improve visual guidance during non-flight locomotion. For the obligate nectar-eating *M. woermanni*, the presence of a temporal area of high ganglion cell density, affording higher spatial resolution, potentially assists with visual control of their tongue during foraging.

An exception to the rule: the cave-dwelling Egyptian rousette bat has a horizontal streak

Our finding of a horizontal streak in the retina of the Egyptian rousette bat *R. aegyptiacus* refutes our prediction that this cave-dwelling species would have only a concentric temporal area reflecting its occupation of a more enclosed microenvironment. In addition, our results contrast with the absence of a visual streak in the same species reported by Heffner et al. (1991). These authors reported only the presence of a temporal area of high density of retinal ganglion cells and no streak is visible from their topographic map. However, the presence of a pronounced horizontal streak is a consistent feature in the retinas of the three specimens of Egyptian rousette bats analyzed in our study. We suggest these differences between our data and Heffner's reflect differences in sampling protocols. In their analyses, Heffner et al (1999) used sampling grids of 200 x 200 μm in the region of high neuronal density and of 1000 x 1000 μm across the rest of the retina. In our study, we performed a high frequency sampling in the region of high density using the same grid size used by Heffner, but we used a sampling grid of 660 x 660 μm across the rest of retina, which is almost twofold finer than the sampling grid used by Heffner et al. (1999). It is likely that their larger sampling grid did not provide enough resolution to detect the presence of a horizontal streak in this species. Moreover, the smaller counting frame size of 35 x 53 μm used by Heffner et al. (1999) may have been another factor that hindered the identification of the streak in this species. For this species, we used a counting frame of 150 x 150 μm, approximately 12x larger in area than the counting frame used by Heffner et al. (1999), which increases the likelihood to detect variations in neuronal density where gradients are shallow, which is the case for *R. aegyptiacus*. These contrasting results give support to the notion that the definition of an optimized stereological sampling scheme is crucial to detect variations in the density of neurons in retinal wholemounts as highlighted by Wässle et al. (1975), Curcio et al. (1990) and Coimbra et al. (2012, 2014, 2015). Functionally, we suggest that the horizontal streak in *R. aegyptiacus* correlates with its needs to forage in the open after leaving their caves. *R. aegyptiacus* forages for in a wide variety of biomes from savannas to woodland forests (Kwiencinski and Griffiths, 1999) in which the presence of a horizontal streak allows for enhanced resolution across the horizon.

Megachiropteran retinal blueprint: Phylogenetic and ecological factors?

In this study, we found that most megachiropteran species studied have a more or less well developed horizontal visual streak and a temporal area of high ganglion cell density in their retinas. The only exception is *H. monstrosus* which has a single temporal area and no horizontal streak. The presence of a horizontal streak in most species, and a temporal area in all species, of this cohort of megachiropterans indicates that these topographic retinal traits are common features shared by these species. Therefore, we suggest that the combination of a horizontal streak and a temporal area represent a presumed megachiropteran retinal blueprint, from which variations in topographic arrangement of retinal ganglion cell densities are derived to reflect more specific aspects of their behavioral ecology and niche occupation. This was particularly clear in the degree of development of the horizontal streak between species that occur in more open or enclosed environments.

Retinal traits do not appear to provide substantive evidence regarding the phylogenetic relationships of megachiropterans as extensively debated in the literature (Pettigrew 1986; Pettigrew et al., 1989). Whereas the presence of a temporal area of high retinal ganglion cell density is a common trait shared by megachiropterans, many micro chiropterans (Coimbra et al., unpublished data) and indeed many other mammals share this type of retinal specializations. Moreover, megachiropterans and microchiropterans show marked differences in the dorsoventral gradients of retinal ganglion cell density. Megachiropterans have a mostly symmetric dorsoventral change in retinal ganglion cell density due to the presence of a horizontal visual streak. In contrast, microchiropterans have a clear dorsoventral asymmetry, with increased retinal ganglion cell density in the ventral part of the retina (Pettigrew et al., 1988; Coimbra et al., unpublished data). In addition, the presence of a horizontal streak across the nasotemporal axis, which is a common retinal feature of megachiropterans, has not been found in the retinas of strepsirhine primates and microchiropterans that occur in relatively more open environments (DeBruyn et al., 1980;

Pettigrew et al., 1988). Given the malleability of the topographic arrangement of retinal ganglion cell densities associated with different aspects of the behavioral ecology and microhabitat occupation of megachiropterans, microchiropterans, primates, and other mammals, retinal topography does not appear to provide useful clues regarding phylogenetic interrelationships.

Factors influencing the spatial resolving power in African megachiropterans

Eye size, diel activity patterns, microhabitat occupation and active predatory habits represent key factors that influence the levels of spatial resolving power in mammals (Veilleux and Kirk, 2014). Our findings that megachiropteran species that use predominantly more enclosed environments for roosting and foraging (*M. woermanni*, *C. argynnis* and *S. zenkeri*) have the lowest spatial resolving power (~2 cycles/degree) compared to species that roost in more open microenvironments (*E. helvum*; ~4 cycles/degree) supports the notion that luminance is crucial to define the number of receptors and hence specializations to improve resolution or sensitivity (Land and Nilsson, 2012). Consistent with our results, two species of Australian megachiropterans (little flying fox, *Pteropus scapulatus* and the grey-headed flying fox, *P. poliochephalus*), which predominantly roost in exposed branches of tall trees, also show higher levels of spatial resolving power (4 and 5.5. cycles/degree, respectively) (Pettigrew et al., 1988). In addition, our estimates of intermediate levels of spatial resolution (~3 cycles/degree) for megachiropteran species that occur in variety of both enclosed and open microhabitats for roosting and foraging (*E. wahlbergi*, *R. aegyptiacus*, *Epomops franqueti*) relates to variation in the luminance levels these animals will experience.

Interestingly, we found an exception to this general trend. Our estimates of spatial resolving power for *H. monstrosus* (~4 cycles/degree), which also occurs in a variety of enclosed and open environments (Langevin and Barclay, 1990), is similar to the estimates of *E. helvum*. This is intriguing because, in contrast to *E. helvum*, which predominantly roosts in the exposed branches of tall trees in more open environments (DeFrees and Wilson, 1988), *H.*

monstrosus roosts beneath dense foliage cover and would be expected to have lower spatial resolution (Langevin and Barclay, 1990). Veilleux and Kirk (2014) have suggested that reliance on a more faunivorous diet may contribute to more elevated levels of spatial resolution in mammals. According to Langevin and Barcley (1990), *H. monstrosus* can consume meat scraps and attack birds, for which higher spatial resolving power is advantageous. However, it seems unlikely that this minor, carnivorous, aspect of this bat's behavior has influenced the evolution of its eye, but it is possible that the larger head and eye size of *H. monstrosus* has permitted a limited degree of predation by virtue of slightly higher visual resolution compared to other African megachiropterans. In line with this view, megachiropteran species with smaller eye size (i.e. *C. argynnis*, *S. zenkeri* and *M. woermanni*) show the lowest levels of spatial resolution and rely predominantly on plant material and nectar, whereas species with larger eye size (i.e. *E. wahlbergi*) may take advantage of the occasional consumption of insects given their higher spatial resolving power (Acharya, 1992; Nowak, 1994; Weber et al., 2009; Fahr, 2014).

Our estimates of spatial resolving power in African megachiropterans support the idea that eye size rather than peak ganglion cell density represents a crucial factor to define elevated levels of spatial resolution in megachiropterans (Pettigrew et al., 1988). Despite *M. woermanni*, *C. argynnis* and *S. zenkeri* having the highest estimated peak density of retinal ganglion cells (~6,000- 6,500 cells/mm^2), their small eyes (~6 mm) bring spatial resolution to lower levels (~2 cycles/degree). In contrast, *E. wahlbergi* and *R. aegyptiacus* show peak densities of retinal ganglion cells in the same range of the species mentioned above, but their relatively larger eyes (~8- 8.5 mm) contribute to an increase in spatial resolving power (~3 cycles/degree). Consistent with this, we estimated a lower peak density of retinal ganglion cells (~5,000 cells/mm^2) for *E. franqueti* and *H. monstrosus* but resolution in these species is ~3 and 4 cycles/degree, respectively, because of their larger eyes (~9.5 and 12 mm), respectively. However, among the species we examined, one exception is *E. helvum*, which has an eye size (~9.4 mm) similar to *E. franqueti*, but its peak ganglion cell density of ~7,000 cells/mm^2 contributes to higher spatial resolving power (~3.8 cycles/degree). As

discussed above, it is likely that the higher peak density of retinal ganglion cell in *E. helvum* reflects increased luminance in the occupation of more open microhabitats compared to *E. franqueti*.

Visual ecology in African megachiropterans: foraging and predator detection

Most species of megachiropterans rely heavily on a variety of fruit, buds and young leaves for nutrition, but some species are more specialized to eat nectar (i.e. *M. woermanni*) whereas others can consume a more faunivorous diet including insects (i.e. *E. wahlbergi*) and small vertebrates (i.e. *H. monstrosus*) (Langevin and Barclay, 1990; Weber et al, 2009). In an ecological perspective, our estimates of spatial resolving power across the megachiropteran species examined potentially allow the detection of a range of food items or assist with visual control of praxic activities during foraging. For example, in the nectar-eating species, *M. woermanni* (~2 cycles/degree), the minimum target size of ~0.8 mm detectable at distances of 10 cm is reasonable to allow for the discrimination of physical features of banana inflorescences (~1-2 cm diameter), thus assisting with visual control of their tongue during foraging (Fig. 7A). At distances of ~1 m, megachiropteran species with spatial resolving powers of 3 to 4 cycles/degree (i.e. *Eidolon helvum*) can spatially discriminate objects as small as 6 and 4 mm, which potentially allows for the detection of a range of fruit such as bananas (~4 cm diameter) and mangoes (~10 cm diameter) (Fig. 7A).

While foraging or roosting, megachiropterans need to remain vigilant for predators. At presumed distances of 10 m, the megachiropterans with the lowest spatial resolving power (~2 cycles/degree) show a minimum target size of 8 cm, whereas species with intermediate (~3 cycles/degree) and high spatial resolving power (~4 cycles/degree) can potentially discriminate objects as small as 4 to 5 cm. Therefore, at ~10 m, the levels of spatial resolving power estimated for the African megachiropterans studied allow for the detection of potential predators including nocturnal raptors (i.e. spotted eagle owls, ~15 cm front), small carnivores (i.e. African palm civets and genets, ~15 cm front) and humans (i.e. some African

populations who consume megachiropterans as bushmeat, ~45 cm shoulder width) (DeFrees and Wilson, 1988; Kwiescinski and Griffths, 1999) (Fig. 7B). Given optimal conditions of contrast and luminance, these predictions illustrate the potential to discriminate visual features from objects in the environment, thus representing a useful proxy to understanding how African megachiropterans use spatial vision in their behavioral ecology.

ACKNOWLEDGEMENTS

We thank Caroline Kerr and Michael Archer for their invaluable assistance at different stages of the project. We want to express our gratitude to Adhil Bhagwandin and Ngalla Jillani for their assistance during the field trips. We thank the wildlife photographers Malcolm Schuyl, Eyal Bartov and Christophe Lepetit for allowing us to use their simply beautiful megachiropteran photos. We also thank the geographer Luis Barbosa for the immeasurable advice on the use of Arcview software to construct the topographic maps. JPC was supported by SIRF/UIS scholarships at The University of Western Australia and URC postdoctoral fellowship at The University of the Witwatersrand. This work was supported by funding from the National Research Foundation of South Africa (PRM), the Belgian co-operation service (DGD) at the Royal Museum for Central Africa (EG). SPC acknowledges the financial assistance of the West Australian State Government.

CONFLICT OF INTEREST STATEMENT

The authors have no conflict of interest in this study.

ROLE OF AUTHORS

All authors had full access to all the data in the study and take responsibility for the integrity of the data and the accuracy of the data analysis. Study concept and design: JPC, JDP,

CKK, EG, SPC, PRM; Collection of specimens: PRM, JDP, CKK, EG; Collection and acquisition of data: JPC; Analysis and interpretation of the data: JPC; Writing of the manuscript: JPC; Critical revision of the manuscript for important intellectual content: JPC, JDP, CKK, EG, SPC, PRM; Obtained funding: PRM, SPC, EG, JPC.

FIGURE AND TABLE LEGENDS

Figure 1. Diversity of open and enclosed roosting microhabitats occupied by African megachiropterans. *Eidolon helvum* roosting in exposed branches of a tree (A); *Hypsignathus monstrosus* roosting under dense foliage (B); *Rousettus aegyptiacus* roosting in a cave (C); Close up of the head of *Epomophorus wahlbergi* to show the large eyes (D). Photo credits to Malcolm Schuyl (*E. helvum*), Christophe Lepetit (*H. monstrosus*), Eyal Bartov (*R. aegyptiacus*) and Paul Manger (*E. wahlbergi*).

Figure 2. Nissl-stained retinal wholemount of *E. wahlbergi* (A). Note the higher density of retinal neurons in the temporal area (B, C) compared to the nasal (D) and ventral (E) aspects of the horizontal streak. Cytological criteria used to distinguish retinal ganglion cells (gc) from amacrine (a) and glial (g) in high (C) and moderate to low (D, E) density regions within the avascular retinal ganglion cell layer of *E. wahlbergii*. The asterisks depict retinal papillae in the photoreceptor layer which are unique to megachiropterans. Retinal papillae as seen in Differential Interference Contrast (DIC) (F). Scale bars = 2.5 mm in A; 100 μm in B; 20 μm in C-F.

Figure 3. Eyecups showing the tapetum lucidum in *Epomops franqueti* (A) and *Hypsignathus monstrosus* (B). Note that in both species the golden-yellow tapetum lucidum occupies the dorsal fundus of the eyecup. Below the optic disc (od), the choroid is pigmented. T, temporal; V, ventral. Scale bars = 2.5 mm.

Figure 4. Topographic maps showing the distribution of ganglion cells in retinal wholemounts of the African straw-colored bat, *E. helvum* (A); Egyptian rousette bat, *R. aegyptiacus* (B); Franquet's epauletted bat, *E. franqueti* (C) and Wahlberg's epauletted bat, *E. wahlebergi* (D). Numbers on the isodensity lines should be multiplied by 10^3 to express densities in cells/mm^2. The dot within the limits of the highest isodensity line in each map marks the location of the peak density of retinal ganglion cells. The black circle in the center of the retina indicates the position of the optic disc. T, temporal; V, ventral. Scale bars= 1 mm.

Figure 5. Topographic maps showing the distribution of ganglion cells in retinal wholemounts of the African long-tongued bat, *M. woermanni* (A); Short-palated bat, *C. argynnis* (B); Zenker's bat, *S. zenkeri* (C) and Hammer-headed bat, *H. monstrosus* (D). Numbers on the isodensity lines should be multiplied by 10^3 to express densities in cells/mm^2. The dot within the limits of the highest isodensity line in each map marks the location of the peak density of retinal ganglion cells. The black circle in the center of the retina indicates the position of the optic disc. T, temporal; V, ventral. Scale bars= 1 mm.

Figure 6. Summary of the patterns of topographic distribution of retinal ganglion cells, spatial resolving power and their relationship with roosting microhabitat occupation among megachiropterans examined in the present study. Variances in topographic densities of ganglion cells are depicted by gray gradient variations.

Figure 7. Schematic diagrams illustrating the minimum target size that representative megachiropterans with varying levels of spatial resolving power can detect at presumed distances relevant for foraging (A) and predator detection (B). Megachiropterans and African palm civet profiles were redrawn from Kingdon (2004).

Table 1. Roosting microhabitat preferences and trophic specializations of the eight megachiropteran species examined.

Table 2. Stereological parameters defined to estimate the total number and topographic distribution of ganglion cells in the retinas of megachiropterans the optical fractionator method.

Table 3. Estimates of the total numbers (rounded to the nearest 1,000) and peak density of ganglion cells obtained from retinal wholemounts of the megachiropteran species studied using the optical fractionator method.

Table 4. Mean Schaeffer Coefficient of Error (CE), Coefficient of Variation (CV) and ratio CE^2/CV^2 derived from estimates of the total number of ganglion cells in megachiropteran retinal wholemounts using the optical fractionators method. SD, standard deviation.

Table 5. Optical and anatomical parameters used to estimate the upper limits of spatial resolving power in the temporal area of the megachiropterans studied. PND, posterior nodal distance; RMF, retinal magnification factor.

Table 6. Minimum resolvable angle and minimum target size estimated using the upper limits of spatial resolving power in the temporal area of the megachiropterans studied. Presumed distances from resolvable objects are based on the needs for foraging and predator detection.

REFERENCES

Acharya L (1992) *Epomophorus wahlbergi*. Mammalian Species 394:1-4.

Beasley N, Graydon M, Giorgi P (1985) Topography of the retinal ganglion cell layer and choroid in two species of flying foxes (Megachiroptera). Neuroscience Letters supplement 19:S39.

Coimbra JP, Collin SP, Hart NS (2014a) Topographic specializations in the retinal ganglion cell layer correlate with lateralized visual behavior, ecology, and evolution in cockatoos. J Comp Neurol 522:3363-3385.

Coimbra JP, Collin SP, Hart NS (2014b) Topographic specializations in the retinal ganglion cell layer of Australian passerines. The Journal of Comparative Neurology.

Coimbra JP, Collin SP, Hart NS (2015a) Variations in retinal photoreceptor topography and the organization of the rod-free zone reflect behavioral diversity in Australian passerines. J Comp Neurol.

Coimbra JP, Hart NS, Collin SP, Manger PR (2013) Scene from above: Retinal ganglion cell topography and spatial resolving power in the giraffe (*Giraffa camelopardalis*). J Comp Neurol 521:2042-2057.

Coimbra JP, Kaswera-Kyamakya C, Gilissen E, Manger PR, Collin SP (2015b) The Retina of Ansorge's Cusimanse (*Crossarchus ansorgei*): Number, Topography and Convergence of Photoreceptors and Ganglion Cells in Relation to Ecology and Behavior. Brain Behav Evol 86:79-93.

Coimbra JP, Marceliano MLV, Andrade-da-Costa BLS, Yamada ES (2006) The retina of tyrant flycatchers: topographic organization of neuronal density and size in the ganglion cell layer of the great kiskadee *Pitangus sulphuratus* and the rusty margined flycatcher *Myiozetetes cayanensis* (Aves : Tyrannidae). Brain Behav Evol 68:15-25.

Coimbra JP, Nolan PM, Collin SP, Hart NS (2012) Retinal ganglion cell topography and spatial resolving power in penguins. Brain Behav Evol 80:254-268.

Coimbra JP, Trévia N, Marceliano MLV, Andrade-da-Costa BLS, Picanço-Diniz CW, Yamada ES (2009) Number and distribution of neurons in the retinal ganglion cell layer in relation to foraging behaviors of tyrant flycatchers. J Comp Neurol 514:66-73.

Collin SP (1999) Behavioural ecology and retinal cell topography. In: Adaptive mechanisms in the ecology of vision(Archer, S. N. et al., eds), pp 509-535 London: Chapman and Hall.

Curcio CA, Allen KA (1990) Topography of ganglion cells in human retina. J Comp Neurol 300:5-25.

Curcio CA, Sloan KR, Kalina RE, Hendrickson AE (1990) Human photoreceptor topography. J Comp Neurol 292:497-523.

DeBruyn E, Wise V, Casagrande V (1980) The size and topographic arrangement of retinal ganglion cells in the galago. Vision Res 20:315-327.

DeFrees SL, Wilson DE (1988) *Eidolon helvum*. Mammalian Species 312:1-5.

Fahr J (2013) *Scotonycteris zenkeri* Zenker's fruit bat. In: Mammals of Africa, vol. IV: Hedgehogs, Shrews and Bats (Happold, M. and Happold, D. C. D., eds), pp 297-299 London: Bloomsbury.

Glaser EM, Wilson PD (1998) The coefficient of error of optical fractionator population size estimates: a computer simulation comparing three estimators. J Microsc 192:163-171.

Gundersen HJG (1977) Notes on the estimation of the numerical density of arbitrary profiles: the edge effect. J Microsc 111:219-223.

Hanke FD, Peichl L, Dehnhardt G (2009) Retinal Ganglion Cell Topography in Juvenile Harbor Seals (*Phoca vitulina*). Brain Behav Evol 74:102-109.

Heffner RS, Koay G, Heffner HE (1999) Sound localization in an old-world fruit bat (*Rousettus aegyptiacus*): Acuity, use of binaural cues, and relationship to vision. J Comp Psychol 113:297.

Heffner RS, Koay G, Heffner HE (2008) Sound localization acuity and its relation to vision in large and small fruit-eating bats: II. Non-echolocating species, *Eidolon helvum* and *Cynopterus brachyotis*. Hear Res 241:80-86.

Hughes A (1977) The topography of vision in mammals of contrasting life style: comparative optics and retinal organisation. F. Crescitelli (ed): Handbook of Sensory Physiology, Vol. VII/5: The Visual System of Vertebrates. Berlin: Springer Verlag, pp. 613-756.

Hughes A (1981) Population magnitudes and distribution of the major modal classes of cat retinal ganglion cell as estimated from HRP filling and a systematic survey of the soma diameter spectra for classical neurones. J Comp Neurol 197:303-339.

Jones C (1972) Comparative ecology of three pteropid bats in Rio Muni, West Africa. J Zool 167:353-370.

Kunz TH, Lumdsen LF (2003) Ecology of cavity and foliage roosting Bats. In: Bat ecology(Kunz, T. H. and Fenton, M. B., eds), pp 3-69 United States: The University of Chicago Press.

Kwiecinski GG, Griffiths TA (1999) *Rousettus egyptiacus*. Mammalian Species 611:1-9.

Langevin P, Barclay RM (1990) *Hypsignathus monstrosus*. Mammalian Species 357:1-4.

Marshall NJ (2000) Communication and camouflage with the same 'bright'colours in reef fishes. Philos Trans R Soc Lond B Biol Sci 355:1243-1248.

Mass AM, Supin AY (1992) Peak density, size and regional distribution of ganglion cells in the retina of the Fur Seal *Callorhinus ursinus*. Brain Behav Evol 39:69-76.

Mass AM, Supin AY (2010) Retinal ganglion cell layer of the caspian seal *Pusa caspica*: topography and localization of the high-resolution area. Brain Behav Evol 76:144-153.

Müller B, Goodman SM, Peichl L (2007) Cone photoreceptor diversity in the retinas of fruit bats (Megachiroptera). Brain Behav Evol 70:90-104.

Peichl L (1992) Topography of ganglion cells in the dog and wolf retina. J Comp Neurol 324:603-620.

Pettigrew J, Jamieson B, Robson S, Hall L, McAnally K, Cooper H (1989) Phylogenetic relations between microbats, megabats and primates (Mammalia: Chiroptera and Primates). Philos Trans R Soc Lond, Ser B: Biol Sci 325:489 - 559.

Pettigrew JD (1986) Flying primates? Megabats have the advanced pathway from eye to midbrain. Science 231:1304-1306.

Pettigrew JD, Dreher B, Hopkins CS, McCall MJ, Brown M (1988) Peak density and distribution of ganglion cells in the retinae of microchiropteran bats: implications for visual acuity. Brain Behav Evol 32:39-56.

Reuter T, Peichl L (2008) Structure and function of the retina in aquatic tetrapods. In: Sensory Evolution on the Threshold–Adaptations in Secondarily Aquatic Vertebrates (Thewissen JGM, Nummela S, eds) pp.149-172.

Nowak RM (1994) Walker's bats of the world. Baltimore: The Johns Hopkins University Press.

Silveira L, Perry V, Yamada E (1993) The retinal ganglion cell distribution and the representation of the visual field in area 17 of the owl monkey, *Aotus trivirgatus*. Vis Neurosci 10:887-897.

Silveira L, Picanço-Diniz C, Sampaio L, Oswaldo-Cruz E (1989a) Retinal ganglion cell distribution in the cebus monkey: a comparison with the cortical magnification factors. Vision Res 29:1471-1483.

Silveira LCL, Picanço-Diniz CW, Oswaldo-Cruz E (1989b) Distribution and size of ganglion cells in the retinae of large Amazon rodents. Vis Neurosci 2:221-235.

Slomianka L, West MJ (2005) Estimators of the precision of stereological estimates: an example based on the CA1 pyramidal cell layer of rats. Neuroscience 136:757-767.

Snyder AW, Miller WH (1977) Photoreceptor diameter and spacing for highest resolving power. JOSA 67:696-698.

Stone J (1981) The wholemount handbook: a guide to the preparation and analysis of retinal wholemounts: Maitland Publications.

Veilleux CC, Kirk EC (2014) Visual acuity in mammals: effects of eye size and ecology. Brain Behav Evol 83:43–53.

Wässle H (2004) Parallel processing in the mammalian retina. Nature Reviews Neuroscience 5:747-757.

Wässle H, Levick W, Cleland B (1975) The distribution of the alpha type of ganglion cells in the cat's retina. J Comp Neurol 159:419-437.

Wässle H, Peichl L, Boycott BB (1981) Morphology and topography of on-and off-alpha cells in the cat retina. Proc R Soc Lond B Biol Sci 212:157-175.

Weber N, Kalko EK, Fahr J (2009) A first assessment of home range and foraging behaviour of the African long-tongued bat *Megaloglossus woermanni* (Chiroptera: Pteropodidae) in a heterogeneous landscape within the Lama Forest Reserve, Benin. Acta Chiropterologica 11:317-329.

West MJ, Slomianka L, Gundersen HJG (1991) Unbiased stereological estimation of the total number of neurons in the subdivisions of the rat hippocampus using the optical fractionator. The Anatomical Record 231:482-497.

Williams DR, Coletta NJ (1987) Cone spacing and the visual resolution limit. JOSA A 4:1514-1523.

Wong ROL, Wye-Dvorak J, Henry GH (1986) Morphology and distribution of neurons in the retinal ganglion cell layer of the adult tammar wallaby - *Macropus eugenii*. J Comp Neurol 253:1-12.

GRAPHICAL ABSTRACT

We measured the topographic distribution of retinal ganglion cells and the upper limits of spatial resolution in the eyes of eight species of African megachiropterans. Our results indicate that these two parameters reflect roosting microhabitat and feeding preferences across species.

141x140mm (72 x 72 DPI)

Table 1. Roosting microhabitat preferences and trophic specializations of the eight species of megachiropterans examined.

Common name	Scientific name	Average species body mass (g)	Roosting microhabitat	Food item
African straw-colored fruit bat	*Eidolon helvum*; Kerr 1792	260.2	Tall trees, lofts in caves, rocks [(1)]	Fruit, buds, young leaves, flowers, nectar and pollen [(1)]
Egyptian rousette fruit bat	*Rousettus aegyptiacus*; Geoffroy, 1810	142.6	Caves [(2)]	Fruit [(2)]
Franquet's epauletted fruit bat	*Epomops franqueti*; Tomes, 1860	115.1	Forests, woodland, grasslands, mosaic vegetation [(3)]	Fruit [(3)]
Wahlberg's epauletted fruit bat	*Epomophorus wahlbergi*; Sundevall, 1846	75.5	Savannas, woodlands, forest margins [(4)]	Fruit, insects [(4)]
Woermann's fruit bat	*Megaloglossus woermanni*; Pagenstecher, 1885	20.2	Forests, shrubs and trees [(5)]	Nectar [(5)]
Short-palated fruit bat	*Casinycteris argynnis*; Thomas, 1910	29.5	Under dense foliage in tropical forests [(6)]	Fruit [(6)]
Zenker's fruit bat	*Scotonycteris zenkeri*; Matschie, 1894	22.4	Forest fringes, forest gaps and cleared areas [(7)]	Fruit [(7)]
Hammer-headed fruit bat	*Hypsignathus monstrosus*; Allen, 1861	324.6	Forests, swamps, mangroves and palm forests [(8)]	Fruit, meat scavenger [(8)]

(1) DeFrees and Wilson, 1988; (2) Kwiecinski and Griffiths, 1999; (3) Nowak, 1994; (4) Acharya, 1992; (5) Weber et al., 2009; (6) Nowak, 1994; (7) Fahr, 2014; (8) Langevin and Barclay, 1990.

Table 2. Stereological parameters defined to estimate the total number and topographic distribution of ganglion cells in the retinas of megachiropterans using the optical fractionator method.

Species/ Sampling region	Counting frame (µm x µm)	Grid (µm x µm)	Area sampling fraction
E. helvum			
Whole retina	150 x 150	800 x 800	0.0352
Peak region	100 x 100	200 x 200	0.025
R. aegyptiacus			
Whole retina	150 x 150	660 x 660	0.0517
Peak region	100 x 100	200 x 200	0.025
E. franqueti			
Whole retina	150 x 150	780 x 780	0.0370
Peak region	100 x 100	200 x 200	0.025
E. wahlbergi			
Whole retina	150 x 150	700 x 700	0.0459
Peak region	100 x 100	200 x 200	0.025
M. woermanni			
Whole retina	150 x 150	470 x 470	0.1019
Peak region	100 x 100	200 x 200	0.025
C. argynnis			
Whole retina	150 x 150	520 x 520	0.0832
Peak region	100 x 100	200 x 200	0.025
S. zenkeri			
Whole retina	150 x 150	450 x 450	0.1111
Peak region	100 x 100	200 x 200	0.025
H. monstrosus			
Whole retina	150 x 150	1000 x 1000	0.0225
Peak region	100 x 100	200 x 200	0.025

Table 2. Stereological parameters defined to estimate the total number and topographic distribution of ganglion cells in the retinas of megachiropterans using the optical fractionator method.

Species/ Sampling region	Counting frame (µm x µm)	Grid (µm x µm)	Area sampling fraction
E. helvum			
Whole retina	150 x 150	800 x 800	0.0352
Peak region	100 x 100	200 x 200	0.25
R. aegyptiacus			
Whole retina	150 x 150	660 x 660	0.0517
Peak region	100 x 100	200 x 200	0.25
E. franqueti			
Whole retina	150 x 150	780 x 780	0.0370
Peak region	100 x 100	200 x 200	0.25
E. wahlbergi			
Whole retina	150 x 150	700 x 700	0.0459
Peak region	100 x 100	200 x 200	0.25
M. woermanni			
Whole retina	150 x 150	470 x 470	0.1019
Peak region	100 x 100	200 x 200	0.25
C. argynnis			
Whole retina	150 x 150	520 x 520	0.0832
Peak region	100 x 100	200 x 200	0.25
S. zenkeri			
Whole retina	150 x 150	450 x 450	0.1111
Peak region	100 x 100	200 x 200	0.25
H. monstrosus			
Whole retina	150 x 150	1000 x 1000	0.0225
Peak region	100 x 100	200 x 200	0.25

Table 3. Estimates of the total numbers (rounded to the nearest 1,000) and peak density of ganglion cells obtained from retinal wholemounts of the megachiropteran species studied using the optical fractionator method.

Species	Retinal area (mm^2)	Number of sites counted	Estimated total number of retinal ganglion cells	CE	Subsampling area (mm^2)	Number of sites counted	Peak density (cells/mm^2)	CE
E. helvum								
Ehe001R	133.28	222	274,000	0.035	1.62	45	6,900	0.040
Ehe002R	142.86	229	285,000	0.032	1.74	45	6,900	0.027
Mean	138.07	226	279,000	0.034	1.68	45	6,900	0.034
R. aegyptiacus								
Rae001R	87.89	221	157,000	0.032	1.07	28	6,300	0.023
Rae002R	95.37	234	163,000	0.032	1.00	28	5,300	0.031
Rae003R	90.68	227	163,000	0.032	1.14	32	6,900	0.041
Mean	91.31	227	161,000	0.032	1.07	29	6,167	0.032
SD	3.78	7	3,801	0		0.07	2	808
E. franqueti								
Efr001R	119.57	212	204,000	0.030	1.55	45	4,900	0.039
Efr002R	125.38	218	195,000	0.031	1.54	45	5,100	0.028
Efr003R	127.19	220	203,000	0.030	1.44	45	5,000	0.034
Mean	124.05	217	201,000	0.03	1.51	45	5,000	0.03
SD	3.98	4	4,883	0.001	0.06	0	100	0.006
E. wahlbergi								
Ewa001R	91.68	205	177,000	0.034	1.22	33	5,700	0.034
Ewa002L	101.47	226	178,000	0.033	1.16	32	5,200	0.043
Ewa003R	118.09	255	218,000	0.031	1.27	35	6,600	0.038
Mean	103.75	229	191,000	0.03	1.22	33	5,833	0.04
SD	13.35	25	23,116	0.002	0.06	2	709	0.005
M. woermanni								
Mwo001L	41.22	212	90,000	0.036	0.53	15	6,200	0.020
Mwo003L	42.05	218	99,000	0.034	0.52	15	6,300	0.035
Mwo004L	39.11	203	94,000	0.037	0.58	15	6,500	0.023
Mean	40.79	211	94,000	0.036	0.05	15	6,333	0.026
SD	1.52	8	4,808	0.002	0.03	0	153	0.008
C. argynnis								
Car002R	50.33	212	144,000	0.032	0.65	18	6,600	0.044
Car005R	50.44	209	128,000	0.031	0.65	15	6,500	0.020
Car006R	48.74	203	125,000	0.025	0.70	18	6,400	0.041
Mean	49.84	208	132,000	0.029	0.67	17	6,500	0.035
SD	0.95	5	9,897	0.004	0.03	2	100	0.013
S. zenkeri								
Sze001L	39.64	214	90,000	0.028	0.82	23	5,700	0.047
H. monstrosus								
Hmo001R	201.40	214	340,000	0.029	1.94	50	4,800	0.020
Hmo002R	187.36	200	281,000	0.031	1.95	50	5,400	0.025
Mean	194.38	207	310,000	0.03	1.95	50	5,100	0.02

Table 4. Mean Schaeffer Coefficient of Error (CE), Coefficient of Variation (CV), and ratio CE^2/CV^2 derived from estimates of the total number of ganglion cells in megachiropteran retinal wholemounts using the optical fractionator method. SD, standard deviation.

Species/ Specimen	Number of retinal ganglion cells	CE
R. aegyptiacus		
Mean	161,223	0.032
SD	3,801	0.000
$CV^2=SD^2/Mean^2$	0.00056	
CE^2	0.00102	
CE^2/CV^2	1.84	
E. franqueti		
Mean	200,528	0.030
SD	4,883	0.001
$CV^2=SD^2/Mean^2$	0.00059	
CE^2	0.00092	
CE^2/CV^2	1.55	
E. wahlbergi		
Mean	190,867	0.030
SD	23,116	0.002
$CV^2=SD^2/Mean^2$	0.01467	
CE^2	0.00107	
CE^2/CV^2	0.07	
M. woermanni		
Mean	94,325	0.036
SD	4,808	0.002
$CV^2=SD^2/Mean^2$	0.00260	
CE^2	0.00127	
CE^2/CV^2	0.49	
C. argynnis		
Mean	132,303	0.029
SD	9,897	0.004
$CV^2=SD^2/Mean^2$	0.00560	
CE^2	0.00086	
CE^2/CV^2	0.15	

Table 5. Optical and anatomical parameters used to estimate the upper limits of spatial resolving power in the central area of the megachiropterans studied. PND, posterior nodal distance; RMF, retinal magnification factor.

Species/ Specimen	Axial length (mm)	Peak density of ganglion cells (cells/mm^2)	PND (mm)	RMF (mm/deg)	Spatial resolving power - Square array (cycles/deg)	Spatial resolving power - Hexagonal array (cycles/deg)
E. helvum						
Ehe001R	9.7	6,900	5.04	0.088	3.7	3.9
Ehe002R	9.1	6,900	4.75	0.083	3.4	3.7
Mean	9.4	6,900	4.90	0.085	3.5	3.8
R. aegyptiacus						
Rae001R	8.1	6,300	4.22	0.074	2.9	3.1
Rae002R	7.8	5,300	4.05	0.071	2.6	2.8
Rae003R	7.8	6,900	4.06	0.071	2.9	3.2
Mean	7.9	6,167	4.11	0.072	2.8	3.0
SD	0.2	808	0.10	0.002	0.2	0.2
E. franqueti						
Efr001R	9.5	4,900	4.95	0.086	3.0	3.2
Efr002R	9.4	5,100	4.87	0.085	3.0	3.3
Efr003R	9.5	5,000	4.96	0.086	3.1	3.3
Mean	9.5	5,000	4.93	0.086	3.0	3.3
SD	0.1	100	0.05	0.001	0.0	0.0
E. wahlbergi						
Ewa001R	8.3	5,700	4.30	0.075	2.8	3.0
Ewa002L	8.1	5,200	4.23	0.074	2.7	2.9
Ewa003R	9.3	6,600	4.81	0.084	3.4	3.7
Mean	8.5	5,833	4.44	0.078	3.0	3.2
SD	0.6	709	0.32	0.006	0.4	0.4
M. woermanni						
Mwo001L	5.7	6,200	2.94	0.051	2.0	2.2
Mwo003L	5.8	6,300	3.04	0.053	2.1	2.3
Mwo004L	5.5	6,500	2.87	0.050	2.0	2.2
Mean	5.7	6,333	2.95	0.051	2.0	2.2
SD	0.2	153	0.08	0.001	0.0	0.1
C. argynnis						
Car002R	6.4	6,600	3.31	0.058	2.3	2.5
Car005R	6.4	6,500	3.31	0.058	2.3	2.5
Car006R	6.2	6,400	3.24	0.057	2.3	2.4
Mean	6.3	6,500	3.28	0.057	2.3	2.5
SD	0.1	100	0.04	0.001	0.0	0.0
S. zenkeri						
Sze001L	6.0	5,700	3.14	0.055	2.1	2.2
H. monstrosus						
Hmo001R	11.9	4,800	6.16	0.107	3.7	4.0
Hmo002R	11.8	5,400	6.15	0.107	3.9	4.2
Mean	11.8	5,100	6.15	0.107	3.8	4.1

Table 6. Minimum resolvable angle and minimum target size estimated using the upper limits of spatial resolving power in the temporal area of the megachiropterans studied. Presumed distances from resolvable objects are based on the needs for foraging and predator detection.

Species	Spatial resolving power (cycles/deg)	Minimum resolvable angle (deg)	Distance from object (m)/ Minimum target size (mm)		
			0.1 m	1 m	10 m
Megaloglossus woermanni	2.2	0.455	0.8	8	80
Scotonyceteris zenkeri	2.2	0.455	0.8	8	80
Casynicteris argynnis	2.5	0.400	0.7	7	70
Rousettus aegyptiacus	3.0	0.333	0.6	6	60
Epomophorus wahlbergi	3.2	0.313	0.5	5	50
Epomops franqueti	3.3	0.303	0.5	5	50
Eidolon helvum	3.8	0.263	0.5	5	50
Hypsignathus monstrosus	4.1	0.244	0.4	4	40

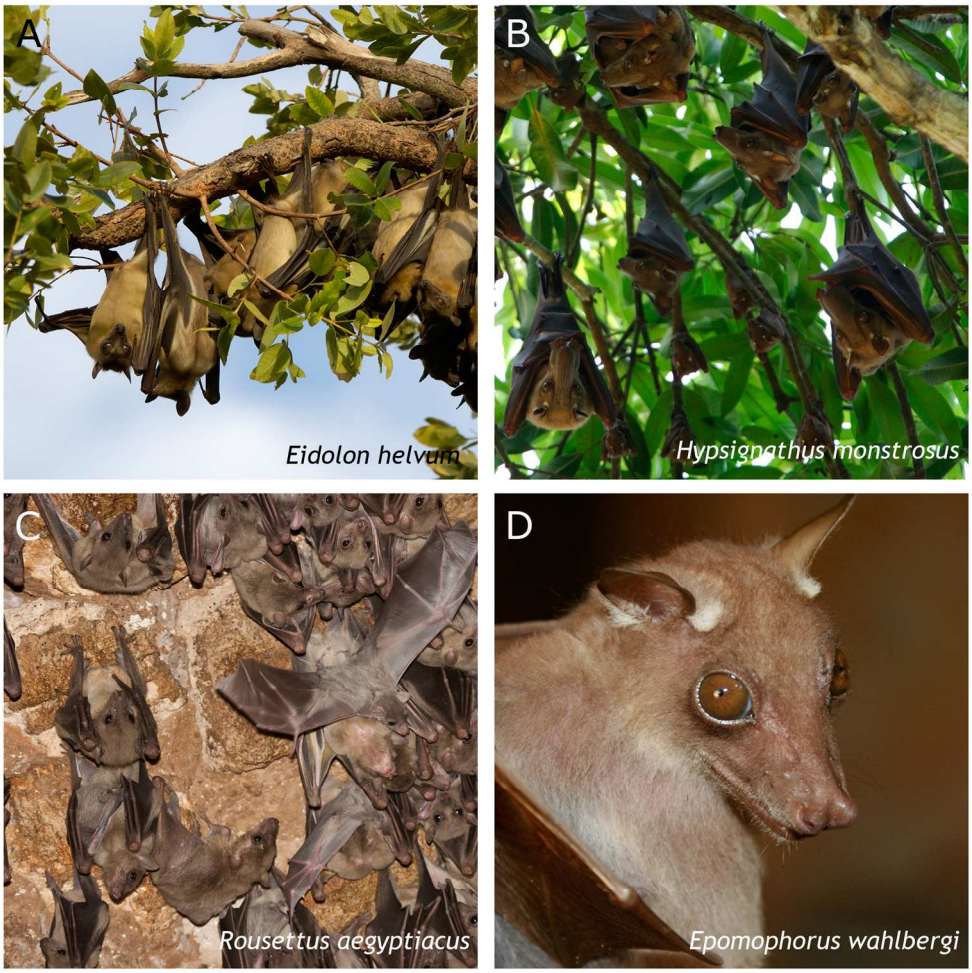

Fig. 1: Diversity of open and enclosed roosting microhabitats occupied by African megachiropterans. Eidolon helvum roosting in exposed branches of a tree (A); Hypsignathus monstrosus roosting under dense foliage (B); Rousettus aegyptiacus roosting in a cave (C); Close up of the head of Epomophorus wahlbergi to show the large eyes (D). Photo credits to Malcolm Schuyl (E. helvum), Christophe Lepetit (H. monstrosus), Eyal Bartov (R. aegyptiacus) and Paul Manger (E. wahlbergi).
168x168mm (300 x 300 DPI)

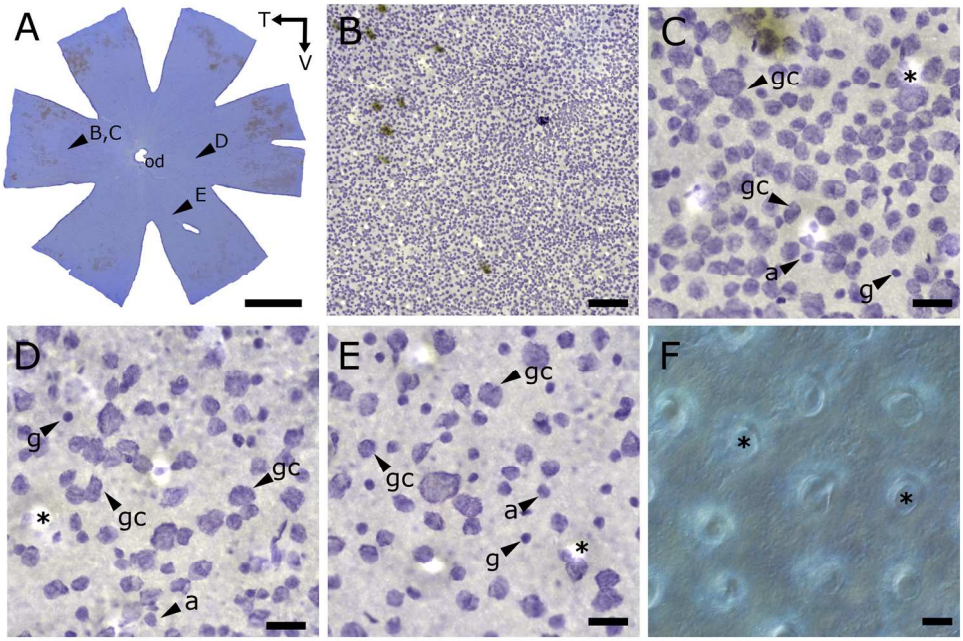

Nissl-stained retinal wholemount of E. wahlbergi (A). Note the higher density of retinal neurons in the temporal area (B, C) compared to the nasal (D) and ventral (E) aspects of the horizontal streak. Cytological criteria used to distinguish retinal ganglion cells (gc) from amacrine (a) and glial (g) in high (C) and moderate to low (D, E) density regions within the avascular retinal ganglion cell layer of E. wahlbergii. The asterisks depict retinal papillae in the photoreceptor layer which are unique to megachiropterans. Retinal papillae as seen in Differential Interference Contrast (DIC) (F). Scale bars = 2.5 mm in A; 100 µm in B; 20 µm C-F.
170x113mm (300 x 300 DPI)

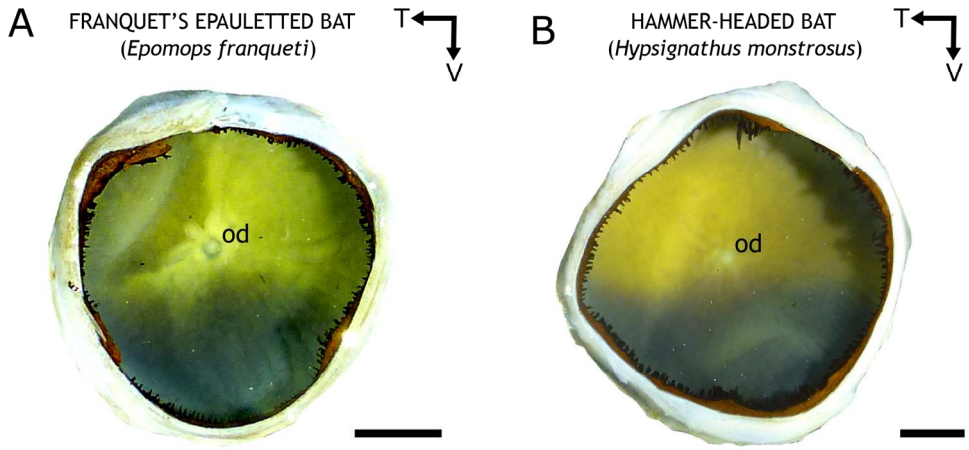

Eyecups showing the tapetum lucidum in Epomops franqueti (A) and Hypsignathus monstrosus (B). Note that in both species the golden-yellow tapetum lucidum occupies the dorsal fundus of the eyecup. Below the optic disc (od), the choroid is pigmented. T, temporal; V, ventral. Scale bars = 2.5 mm.
166x83mm (300 x 300 DPI)

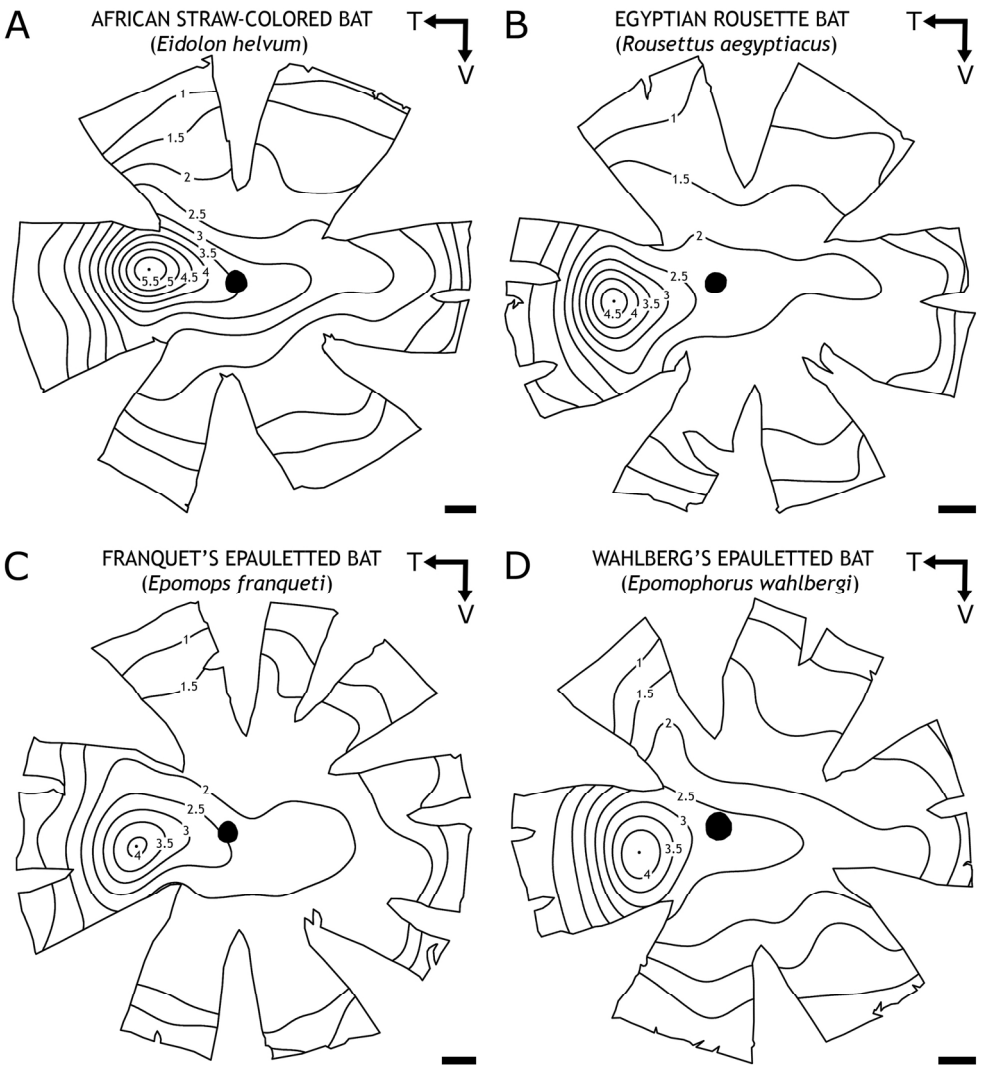

Fig. 4: Topographic maps showing the distribution of ganglion cells in retinal wholemounts of the African-straw colored bat, E. helvum (A); Egyptian rousette bat, R. aegyptiacus (B); Franquet's epauletted bat, E. franqueti (C) and Wahlberg's epauletted bat, E. wahlebergi (D). Numbers on the isodensity lines should be multiplied by 103 to express densities in cells/mm2. The dot within the limits of the highest isodensity line in each map marks the location of the peak density of retinal ganglion cells. The black circle in the center of the retina indicates the position of the optic disc. T, temporal; V, ventral. Scale bars= 1 mm.
170x186mm (300 x 300 DPI)

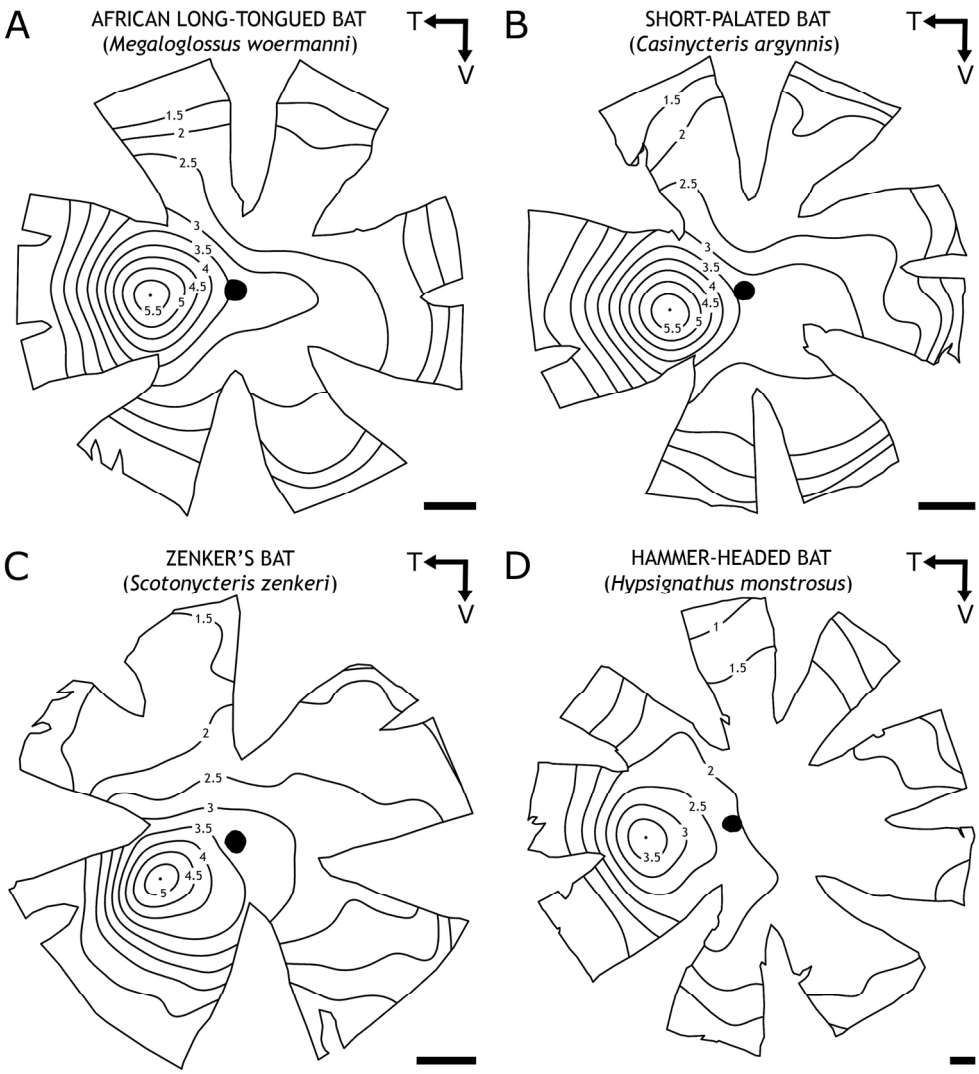

Fig. 5: Topographic maps showing the distribution of ganglion cells in retinal wholemounts of the African long-tongued bat, M. woermanni (A); Short-palated bat, C. argynnis (B); Zenker's bat, S. zenkeri (C) and Hammer-headed bat, H. monstrosus (D). Numbers on the isodensity lines should be multiplied by 103 to express densities in cells/mm2. The dot within the limits of the highest isodensity line in each map marks the location of the peak density of retinal ganglion cells. The black circle in the center of the retina indicates the position of the optic disc. T, temporal; V, ventral. Scale bars= 1 mm.
170x187mm (300 x 300 DPI)

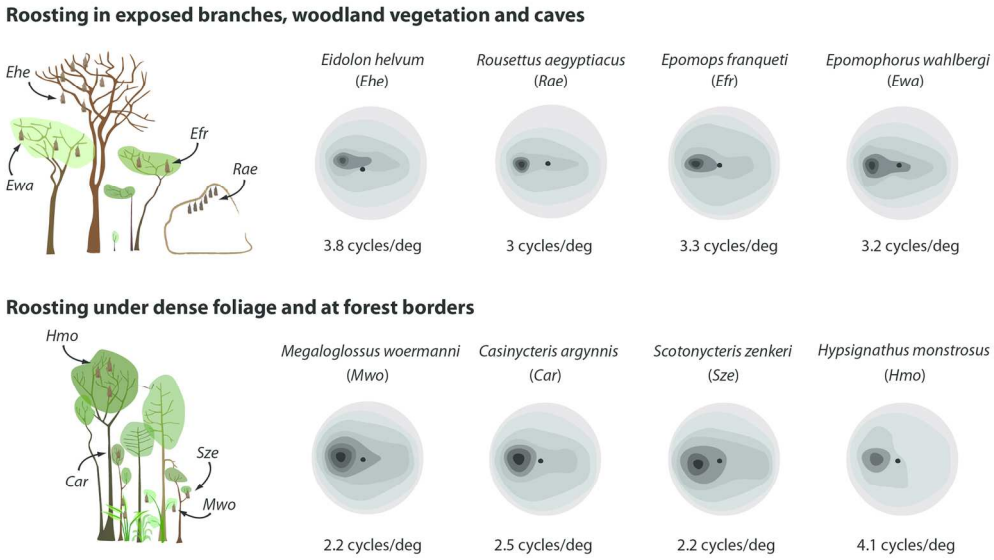

Fig. 6: Summary of the patterns of topographic distribution of retinal ganglion cells, spatial resolving power and their relationship with roosting microhabitat occupation among megachiropterans examined in the present study. Variances in topographic densities of ganglion cells are depicted by gray gradient variations.
170x101mm (300 x 300 DPI)

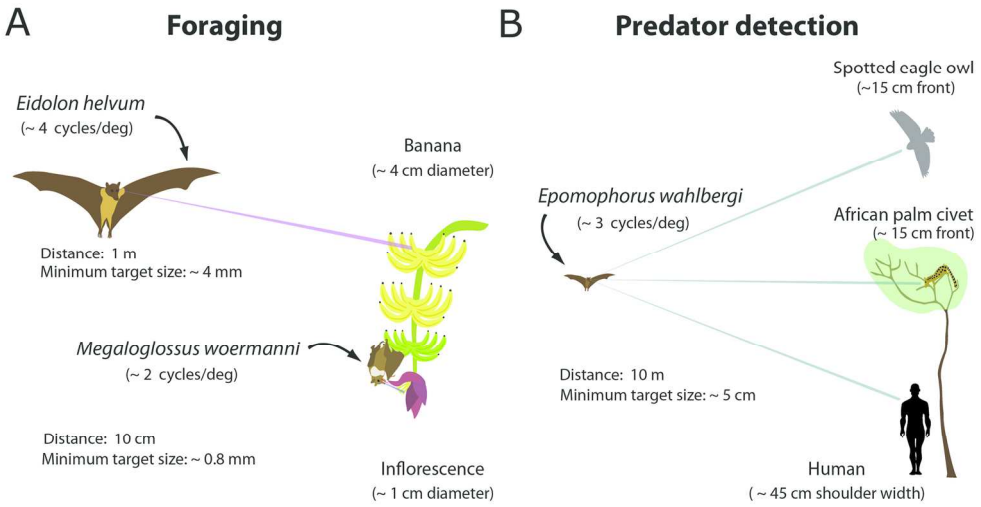

Schematic diagrams illustrating the minimum target size that representative megachiropterans with varying levels of spatial resolving power can detect at presumed distances relevant for foraging (A) and predator detection (B). Megachiropterans and African palm civet profiles were redrawn from Kingdon (2004).
169x93mm (300 x 300 DPI)